

See discussions, stats, and author profiles for this publication at: <https://www.researchgate.net/publication/266677370>

Preparation of melanin from *Catharsius molossus* L. and preliminary study on its chemical structure

ARTICLE *in* JOURNAL OF BIOSCIENCE AND BIOENGINEERING · OCTOBER 2014

Impact Factor: 1.88 · DOI: 10.1016/j.jbiosc.2014.09.009

CITATIONS

2

READS

42

8 AUTHORS, INCLUDING:



Chao Xin

Harbin Institute of Technology

4 PUBLICATIONS 5 CITATIONS

SEE PROFILE



Preparation of melanin from *Catharsius molossus* L. and preliminary study on its chemical structure

Chao Xin,^{1,*} Jia-hua Ma,¹ Cheng-jia Tan,² Zhou Yang,¹ Feng Ye,¹ Chan Long,¹ Shuang Ye,¹ and Da-bin Hou¹

Engineering Research Center for Biomass Resource Utilization and Modification of Sichuan Province, Southwest University of Science and Technology, Mianyang 621010, China¹ and Mianyang Normal University, Mianyang 62100, China²

Received 19 May 2014; accepted 13 September 2014
Available online xxx

A great deal of melanin was found in the waste alkali liquor produced by extraction of chitin from *Catharsius molossus* L. Discarding the lye could harm the environment and cause waste of resources. In this paper, melanin from *C. molossus* L. was recovered through acid precipitation and purified by pepsin and so on. The purity, chemical composition and structure of the prepared melanin were explored by UV-visible absorption spectroscopy, Fourier transform infrared spectroscopy, proton nuclear magnetic resonance spectroscopy, high resolution ¹³C Cross polarization magic angle spinning nuclear magnetic resonance spectroscopy, pyrolysis gas chromatography mass spectrometry, X ray diffraction, X ray fluorescence, matrix-assisted laser desorption/ionization time of flight tandem mass spectrometry, thermal analysis, and so on. The results showed that the purity of the prepared melanin was higher than the commercial standard melanin and it was a kind of nanoaggregates composed of a large quantity of 5,6-dihydroxyindole eumelanin and a small amount of phaeomelanin. In addition, the prepared melanin was irregular in shape and its structure could be divided into three levels: advanced structure maintained by polypeptides, substructure maintained by the ferric ion and microstructure. In particular, the smallest structural unit showed the graphite-like layered structure containing five layers linked by non-covalent bonds and each layer mainly consisted of 5,6-dihydroxyindole and its derivatives, which might be connected to each other through various chemical bonds.

© 2014, The Society for Biotechnology, Japan. All rights reserved.

[Key words: *Catharsius molossus* L.; Melanin; Preparation; Preliminary; Chemical structure]

Melanin is widely present in animals and plants, mainly composed of eumelanin and phaeomelanin. The main chemical monomers of eumelanin are 5,6-dihydroxyindole (DHI) and 5,6-dihydroxyindole-2-carboxylic acid (DHICA) instead of benzothiazine and benzothiazole in phaeomelanin (1). The exploration of melanin structure has been hindered by melanin characters of paramagnetism, amorphism, chemical insoluble and structural diversity, leading to the uncertain chemical composition and structure (2), which prevents the development and utilization of melanin resources.

Natural melanin showed a broad spectrum of biological roles, including antioxidant (3), antitumor activity (4), antivenin activity (5), anti-virus (6), liver protecting activity (7) and radio protective (8) and so on. It has been widely used in medicine, pharmacology, cosmetics and other fields. Recently, natural melanin from different organisms such as squid, black-bone silky fowl, fungi mammals, amphibians and fossils has been studied. However, melanin from these sources was difficult to be developed and promoted due to lower content and higher cost. Black insect resources were rich and there was much melanin in the bodies of black insects. Unfortunately, few studies were focused on the development of insect melanin. *C. molossus* L. belonging to the family scarabaeidae was the important Chinese herbal medicine, whose polypeptide was a

major component of the treatment of benign prostatic hyperplasia (9). Prophase research indicated some chitin existed in the residue of *C. molossus* L. after the extraction of polypeptide (10) and a great deal of melanin was present in the waste alkali liquor produced by extraction of chitin. Based on the problems above, the high-purity *C. molossus* L. melanin was prepared from the waste alkali liquor. Further, preliminary study on the chemical composition and structure of melanin from *C. molossus* L. was conducted by proton nuclear magnetic resonance spectroscopy (¹H NMR), high resolution ¹³C cross polarization magic angle spinning nuclear magnetic resonance spectroscopy (¹³C CP HRMAS NMR), pyrolysis gas chromatography mass spectrometry (Py-GC/MS), X ray diffraction (XRD), X ray fluorescence (XRF), matrix-assisted laser desorption/ionization time of flight tandem mass spectrometry (MALDI-TOF/TOF-MS), thermal analysis, and so on. This study could provide the theoretical basis and technical support for the potential utilization of melanin from *C. molossus* L.

MATERIALS AND METHODS

Materials *Sepia* melanin was obtained from Sigma–Aldrich Co. (Shanghai, China); *C. molossus* L. was purchased from lotus pond medicine market, Chengdu, China.

Reagents and instruments The pepsin (BR, 1200 μg) was purchased from Sinopharm Chemical Reagent Co., Ltd. (Shanghai, China). Other analytical reagents were purchased from Chengdu Kelong Chemical Reagent Co., Ltd. (Chengdu, China). Large-capacity low-speed centrifuge (Shanghai Feige Electric Factory, China); LGJ 240 freeze dryer (Thermo Fisher Scientific Inc., USA); TU-1900 UV–Vis

* Corresponding author. Tel.: +86 816 6089531; fax: +86 816 6089523.
E-mail address: xinchao198811@126.com (C. Xin).

spectrophotometer (Beijing Purkinje General Instrument Co., Ltd., China); Spectrum One (Version BM) Fourier transform infrared spectrometer (PerkinElmer Inc., USA); SDT Q600 simultaneous thermal analyzer (TA Instruments, USA); Vario EL CUBE (Elemental Analysis Systems, Inc., Germany); Bruker Avance III 600 nuclear magnetic resonance spectrometer (Bruker Co., Germany); Bruker Avance III 400 nuclear magnetic resonance spectrometer (Bruker Co., Germany); QP2010 PLUS Pyrolysis-GC/MS (Shimadzu Co., Japan); UltrafleXtreme MALDI-TOF-MS (Bruker Co.); X'Pert PRO XRD (PANalytical B.V., The Netherlands); Axios XRF (PANalytical B.V., Holland); Ultra 55 field emission scanning electronic microscope (FSEM) (Zeiss Co., Germany).

Preparation and purification of melanin from *C. molossus* L. The chitin from *C. molossus* L. was extracted according to previous method (10). Briefly, the residue of *C. molossus* L. after the extraction of polypeptide was successively demineralized and deproteinized by 1.3 M hydrochloric acid and 4 M sodium hydroxide solution. Collected the filtrate of deproteinization and removed the impurities by air pump filtration. The filtrate was adjusted to pH 2.0 with 6 M hydrochloric acid, and centrifuged at 6000 rpm for 15 min after standing at room temperature for 12 h. The precipitate was washed with deionized water until its pH was 7 and lyophilized to obtain crude melanin. Further, purified by washing successively with petroleum ether, ethyl acetate, acetone and deionized water. Next, the melanin was dispersed in deionized water with pH 2, adding an appropriate amount of pepsin (12 μ g/ml), stirring for 48 h at 37°C. Finally, centrifuged at 6000 rpm for 15 min after enzymatic hydrolysis, the precipitate was washed with deionized water (8 times) and lyophilized to obtain purified melanin.

Determination of melanin content *Sepia* melanin and melanin from *C. molossus* L. solubilized in 0.05 M sodium hydroxide solution were analyzed for absorbance at 500 nm to determine total melanin content. Standard curve of *Sepia* melanin was constructed using 0, 20, 40, 60, 80 and 90 mg/l melanin (where C is mass concentration and A is the absorbance). The solution of purified melanin from *C. molossus* L. was prepared and the total melanin content was measured (its purity was represented by the purity of *Sepia* melanin). Finally, the $A_{650\text{nm}}$ values of *Sepia* melanin and purified melanin from *C. molossus* L. solutions with certain concentrations were measured respectively and the $A_{650\text{nm}}/A_{500\text{nm}}$ ratios were calculated to estimate the eumelanin/total melanin ratio in the *C. molossus* L. melanin.

Pyrolysis gas chromatography mass spectrometry *Sepia* melanin and purified melanin from *C. molossus* L. were respectively analyzed by Py-GC/MS. The parameters were as follows: The pyrolyzer was heated to 615°C at 400°C s⁻¹, held at this temperature for 15 s. Helium carrier gas was at a flow rate of 1.0 mL/min. Pyrolysis chamber was held at 200°C and GC injector was maintained at 250°C, using an AB-5MS capillary column (5% diphenyl-95% dimethylpolysiloxane; 60 m \times 0.25 mm \times 0.25 μ m). The GC oven was operated under the following programme: isothermal for 5 min at 35°C, temperature programmed at 4°C min⁻¹ to 310°C, and then isothermal for 10 min, split ratio 40/1. The mass spectrometer was operated in full scan mode, 70 eV ionization voltage and an ionization source temperature of 200°C.

Elemental analysis Percentages contents of C, H, N, S in the purified melanin from *C. molossus* L. were determined by elemental analyzer with the following conditions: The temperatures of oxidation tube and reduction tube were respectively 1150°C and 850°C. The experiment was carried out in high-purity helium and oxygen atmosphere.

Fourier transform infrared spectroscopy Two mg *Sepia* melanin and purified melanin from *C. molossus* L. were respectively weighed, mixed with 200 mg dry KBr and pressed into tablets, then scanned with the scanning range of 4000–400 cm⁻¹.

¹H NMR and ¹³C CP HRMAS NMR The purified melanin from *C. molossus* L. was dissolved in DMSO-*d*₆. The ¹H NMR experiment was performed with the following conditions: a temperature of 299.0 K and a delay time of 1.000 s, observation spectral width of 8223.685 Hz, sampling repetitions of 16, observation frequency of 400.10 MHz, and the matrix size of 65,536 for the transform data. The chemical shifts of ¹H was externally referenced to TMS.

The purified melanin from *C. molossus* L. solid was directly analyzed by the Bruker AVANCE III 600 spectrometer at a resonance frequency of 150.9 MHz ¹³C CP/MAS NMR spectra were recorded using a 4 mm HRMAS probe and a spinning rate of 8 kHz. A contact time of 2 ms, a recycle delay of 5 s, and 4000 accumulations was used. The chemical shifts of ¹³C were externally referenced to TMS.

X ray diffraction The purified melanin from *C. molossus* L. was analyzed by X ray diffraction with the following parameters: CuK α radiation (λ = 1.5406 Å), voltage 40 kV, current 40 mA, 2 θ range 3°–80°.

X ray fluorescence Elements ranging from F to U in the purified melanin from *C. molossus* L. were analyzed qualitatively by XRF with the voltage 60 kV, current 100 mA. In particular, the normalized value (100%) was the value after removal of the sample loss on ignition.

Field emission scanning electronic microscope The purified melanin from *C. molossus* L. was coated with Au and imaged directly by FSEM. Particle size revealed in the FSEM images was measured by the software. The precision of measurement for the average size was about 0.8 nm.

MALDI-TOF/TOF-MS The purified melanin from *C. molossus* L. was analyzed by MALDI-TOF/TOF-MS in positive ion reflector mode and the matrix was HCCA.

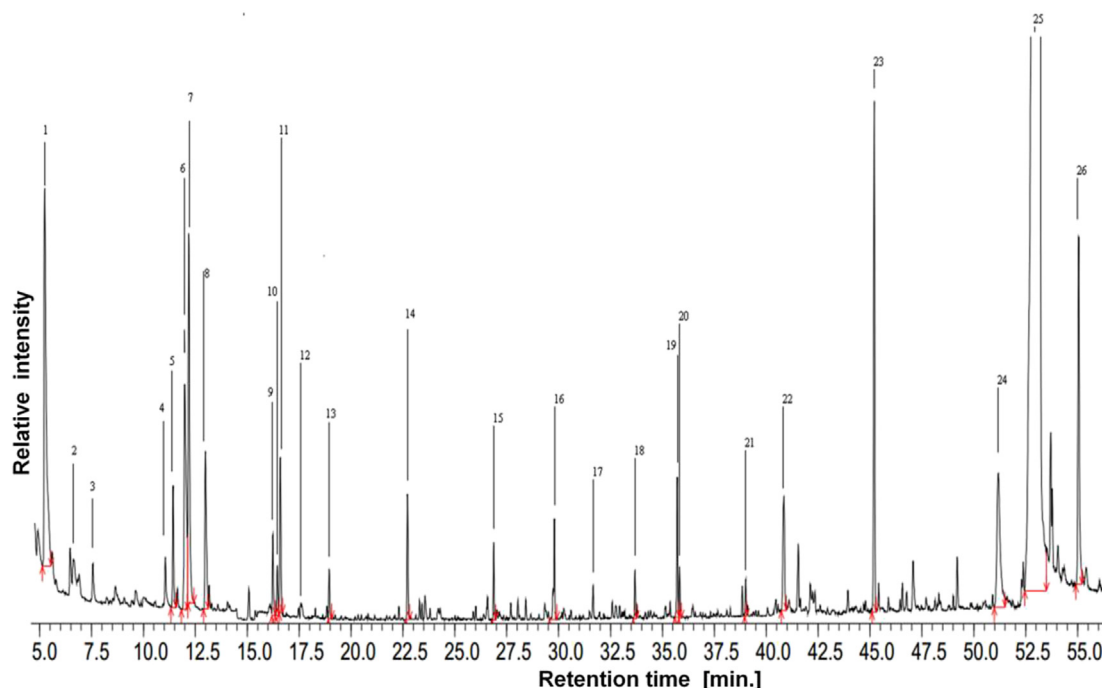
Thermal analysis Purified melanin from *C. molossus* L. (4.2720 mg) was weighed and analyzed by the thermal analyzer. TGA, DSC, DTG data were recorded under an atmosphere of nitrogen, at the flow rate of 50 mL/min. The temperature was from ambient to 600°C at a heating rate of 10°C/min.

RESULTS AND DISCUSSION

Preparation of melanin from *C. molossus* L. Melanin from *C. molossus* L. was prepared using the waste alkali liquor produced by extraction of chitin and was further purified by the organic solvents and pepsin. The bright black, powdered, purified melanin was obtained and its mass was about two percent of the residue of *C. molossus* L. after polypeptide extraction.

Determination of melanin content For the melanin solution with certain concentration, the $A_{500\text{nm}}$ value could be used to quantify the total combined amount of eumelanin and pheomelanin and the ratio $A_{650\text{nm}}/A_{500\text{nm}}$ could serve as a parameter to estimate the eumelanin/total melanin ratio (11). Therefore, the UV–visible absorption spectroscopy was used to determine the content of total melanin and the eumelanin/total melanin ratio in the melanin from *C. molossus* L. Standard curve of *Sepia* melanin ($C = 118.46A_{500\text{nm}} + 1.6484$, $R^2 = 0.9987$) was got within the concentration range from 0 mg/L to 90 mg/L. Further calculated, the content of total melanin from *C. molossus* L. was 103% of that of *Sepia* melanin (Sigma), which indicated the melanin prepared in this paper was in higher purity. The ratio $A_{650\text{nm}}/A_{500\text{nm}}$ of *Sepia* melanin (Sigma) and melanin from *C. molossus* L. were 0.36 and 0.39, respectively. Previous research results showed *Sepia* melanin was eumelanin composed of 75% DHICA and 20% DHI chemical monomers and other substances (12) and the ratio $A_{650\text{nm}}/A_{500\text{nm}}$ of DHI-eumelanin was larger than that of DHICA-eumelanin (11). Herein, it could be inferred that melanin from *C. molossus* L. mainly consisted of eumelanin and contained more DHI chemical monomers than *Sepia* melanin, which was also consistent with the conclusion that insects lacked DHICA-eumelanin (13).

Py-GC/MS analysis Py-GC/MS was the powerful mean to obtain structural information of melanin. The advantages of this technique versus that based on chemical degradation included high sensitivity, specificity and speed, and relatively low risk of possible artifacts (14). Especially, it could effectively distinguish between eumelanin and phaeomelanin (15). Melanin from *C. molossus* L. and *Sepia* melanin were respectively characterized by Py-GC/MS (Figs. 1 and 2). The spectra were explained according to the National Institute of Standards and Technology (NIST) standard library and related literature (16–18). Results of Py-GC/MS (Fig. 3) revealed the pyrolysis products of two kinds of melanin were similar, including toluene [8], pyrrole [7], indole [19], phenol [14] and their alkyl derivatives, which were the characteristic pyrolysis products of eumelanin (19). In addition, traces of alkyl derivatives of thiophene, higher content of indole and its derivatives were detected in the melanin from *C. molossus* L., showing this melanin was composed of a large amount of eumelanin and traces of phaeomelanin and its purity was higher than that of *Sepia* melanin, which was consistent with the conclusion drawn by UV–visible absorption spectroscopy. There were pyridine and its derivatives and structural fragment [5] in the pyrolysis products of two kinds of melanin due to the existence of a small amount of proteins. However, for melanin from *C. molossus* L., pyridine and its derivatives might also be derived from the structure of phaeomelanin (16). Structural fragments [11,21,22] in both melanin showed there was the structure of 5,6-diacetoxy-1-methyl indole in natural melanin, verifying the conjecture of the related literature (20). Structure of 5,6-dipropionyl-1-methyl indole [23] existed merely in the *Sepia* melanin. Further, structural fragments [25,26] with lower content and more

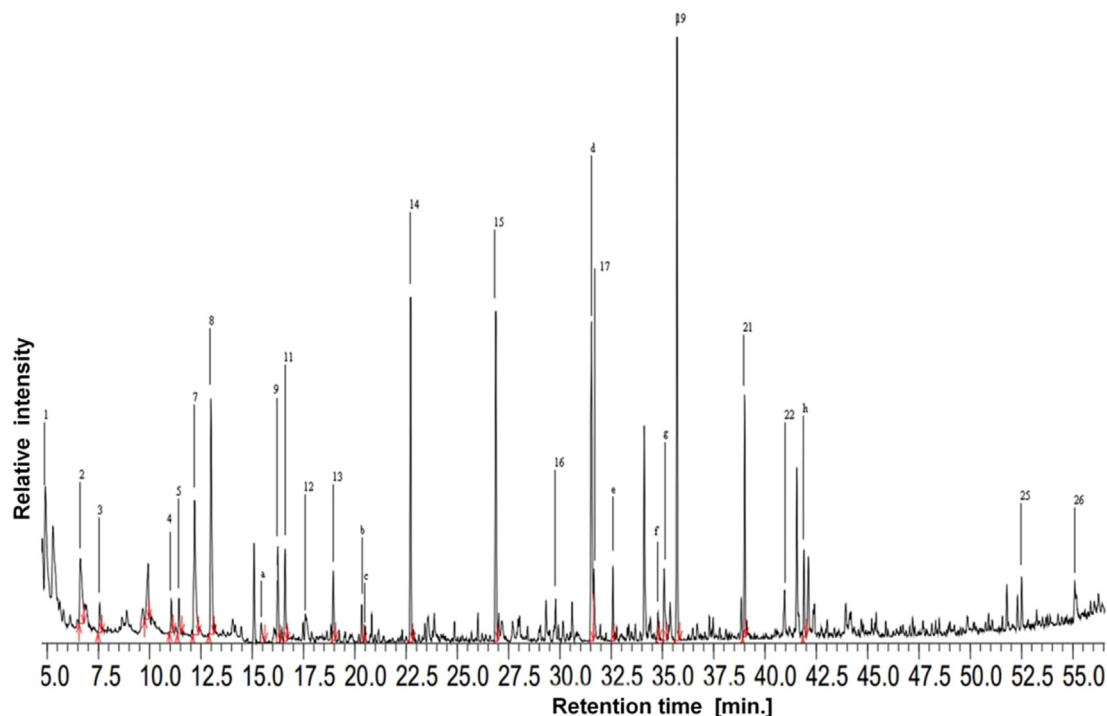
FIG. 1. Total ion chromatogram of *Sepia* melanin.

structural fragments about hydroquinone and derivatives, dioxindoline were detected in the *C. molossus* L. melanin, indicating a smaller amounts of *N*-acetyl-D-galactosamine existed (21) and dioxindoline might coexist with hydroxy indole, uncyclized DOPA in this melanin. Differences between the pyrolysis products of two kinds of melanin showed the chemical composition and structure of heterologous melanin were different.

Elemental analysis The water content of melanin from *C. molossus* L. was about 8% (w/w). Correcting the original elemental

analysis data (w/w) to account for the moisture content gave: C, 60.00%; H, 3.75%; N, 9.18%; and S, 0.54%. Further calculations gave: $C/H_{(mol/mol)} = 1.33$; $C/N_{(mol/mol)} = 7.62$; $S/N_{(mol/mol)} = 0.03$. Particularly, it showed there was traces of phaeomelanin in the melanin from *C. molossus* L. according to S/N value (22).

Fourier transform infrared spectroscopy scanning Fourier transform infrared spectroscopy (FTIR) spectra for melanin from *C. molossus* L. and *Sepia* melanin were similar (Fig. 4) and fit well with established vibrations in the literature (23). A broad band

FIG. 2. Total ion chromatogram of melanin from *Catharsius molossus* L.

Number	Structural fragment	Number	Structural fragment	Number	Structural fragment
1		13		25	
2		14		26	
3		15		a	
4		16		b	
5		17		c	
6		18		d	
7		19		e	
8		20		f	
9		21		g	
10		22		h	
11		23			
12		24			

FIG. 3. The Py-GC/MS products of melanin.

corresponding to phenolic OH stretches was seen at 3400 cm^{-1} . Aliphatic C–H stretches were visible at $2950\text{--}2850\text{ cm}^{-1}$, aromatic C=C stretches and COO stretches were visible at $1650\text{--}1600\text{ cm}^{-1}$ and phenolic COH bends and indolic and phenolic NH stretches were visible at $1400\text{--}1380\text{ cm}^{-1}$. Specifically, the weak absorption peaks at $800\text{--}600\text{ cm}^{-1}$ indicated some positions of aromatic rings were substituted and

the conjugated system with low amount of aromatic hydrogen content was formed. In addition, aliphatic C–C stretches were visible at 1453 cm^{-1} in the melanin from *C. molossus* L., showing there might be a small amount of protein intimately bound to melanin. These results strongly suggested that both *Sepia* and *C. molossus* L. samples were at least partially composed of phenolic rings. Accepted partial structures of melanin included indole and pyrrole rings conjugated to form networks.

^1H NMR and ^{13}C CP HRMAS NMR analysis ^1H NMR result (Fig. 5) showed it was difficult to make the quantitative analysis and estimate spin–spin coupling due to the intramolecular disorders of melanin from *C. molossus* L., but qualitative analysis could be made. In the aliphatic region of the ^1H NMR spectra, signals in the range $0.8\text{--}1.0\text{ ppm}$ could be assigned to CH_3 groups of alkyl fragments, such as CH_2CH_3 , $\text{CH}(\text{CH}_3)_2$, which might come from residual protein; signals at 2.0 ppm belonged to methylene or the ester group ($-\text{OCOCH}_3$) (24), indicating the existence of carboxylate structures. The broad peak in the absorption region around 3.5 ppm could be assigned to methyl ($\text{N}-\text{CH}_3$) bound to the 1st position of indole or pyrrole ring and $-\text{OCH}_3$ bound to the ring (25). The broadened signals centered at 6.5 and 7.3 ppm were aromatic hydrogens of indole or pyrrole ring, showing the various chemical environments around aromatic hydrogens and the diversity of connections among various groups in the melanin from *C. molossus* L. It was worth noting the signals of carboxyl protons were not detected due to the fact that *C. molossus* L. sample was mainly composed of DHI-eumelanin without carboxyl. Particularly, hydrolyzed by pepsin for 48 h , part of protein still existed, suggesting melanin was closely bound to the protein to form the enzyme-resistant structure similar to the shell of adult *C. molossus* L.

A large number of paramagnetic radicals in the melanin from *C. molossus* L. resulted in the broadened ^{13}C CP HRMAS NMR spectra (Fig. 6). The ^{13}C CP HRMAS NMR data collected for *C. molossus* L. sample fit well with published NMR assignments of *Sepia* melanin (26), which was consistent with the conclusion that melanin from *C. molossus* L. mainly consists of eumelanin drawn by Py-GC/MS, IR

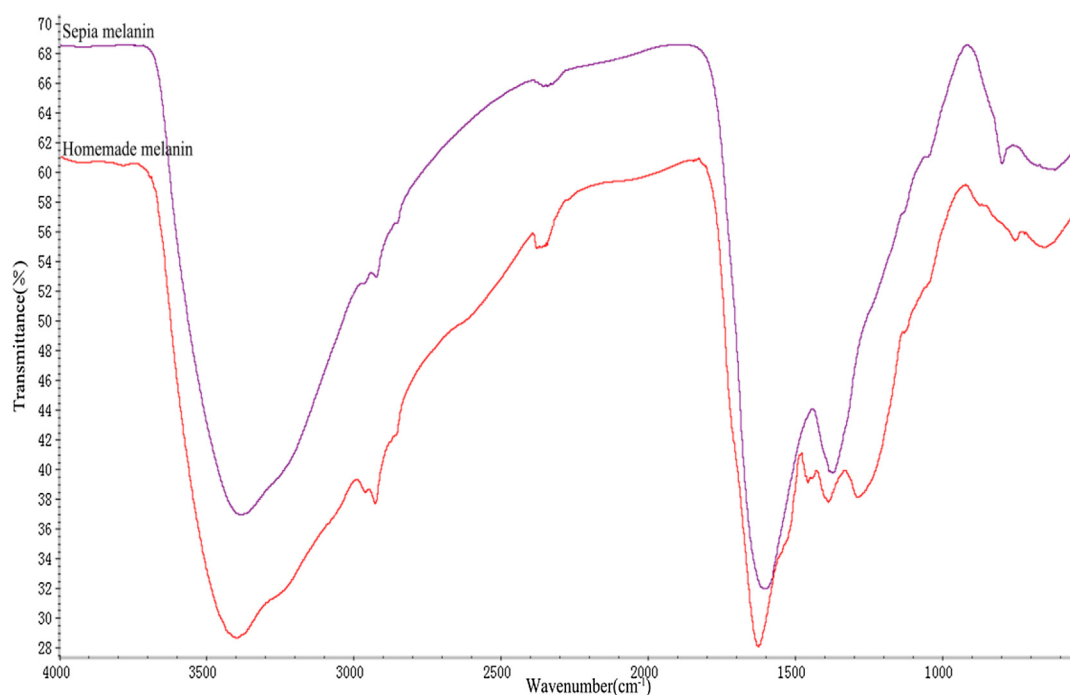
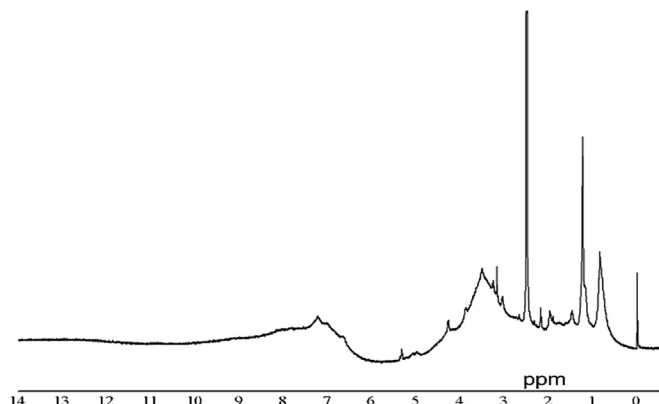
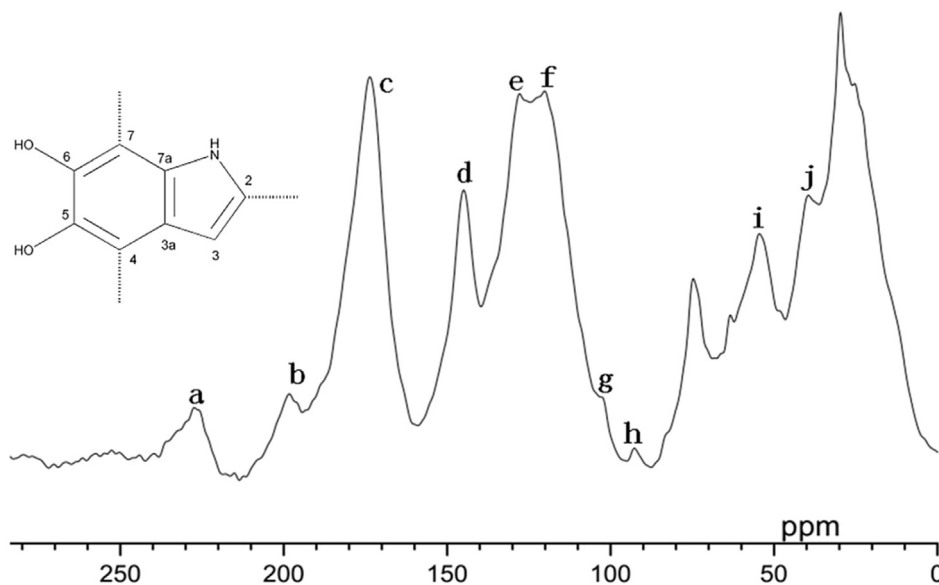


FIG. 4. Infrared spectra of melanin.

FIG. 5. ^1H NMR spectra of melanin from *Catharsius molossus* L.

and so on. The spectra could be divided into three regions: The aliphatic region ($\delta = 10\text{--}95$ ppm), which mainly corresponded to proteins (most likely proteins that constituted the amorphous matrix that embedded eumelanin) that were still associated with melanin after its enzymatic hydrolysis and alkyl, uncyclized L-DOPA bound to melanin. In particular, peaks at 35.2 (j) and 55.7 (i) ppm were assigned as methyl (N-CH_3) bound to the 1st position of indole or pyrrole ring and OCH_3 bound to the ring or CH_2 and CH in the uncyclized L-DOPA (27), respectively. The aromatic region ($\delta = 95\text{--}145$ ppm), which corresponded to indole and pyrrole groups in the melanin. These peaks were not resolved enough to assign every carbon expected in a melanin monomer unit, but the peaks at 145 (peak d), 128 (peak e), 113 (peak f), 102.5 (peak g) ppm fit well with 5-C and 6-C, 7a-C, 3a-C, 3-C in the expected chemical shifts of a melanin monomer as shown in Fig. 6. Particularly, the signals of 7-C (δ 90 ppm) and 4-C (δ 97 ppm) were absent, which might be because most positions of 7-C and 4-C were substituted with the substituents, leading to the upfield chemical shift. The carbonyl region ($\delta = 160\text{--}200$ ppm), which corresponded to backbone carbonyl groups belonging to the peptidic bonds and side-chain carboxyl and amido groups, together with the carbonyl group of the quinone moieties of melanin (typically at about $\delta = 175$ ppm, peak c in Fig. 6). Respectively, the peaks at 195 (peak b) and 230 ppm (peak a) were assigned as unprotonated carboxyl groups (28) and the spinning side band.

FIG. 6. ^{13}C CP HRMAS NMR spectra of melanin from *Catharsius molossus* L.

XRD analysis The XRD spectra at room temperature of melanin from *C. molossus* L. was characterized by a broad peak (as occurred in amorphous and disordered materials), centred at about 24.5° (Fig. 7). Such peak was due to X ray diffraction from parallel planar layers (29).

The peak position could give information about the interlayer spacing d , according to the Bragg equation:

$$2d\sin\theta = m\lambda \quad (1)$$

where θ is the diffraction angle, m is the diffraction order and λ is the X ray wavelength. By considering the first order diffraction ($m = 1$), we obtained $d = 3.6$ Å. In particular, the value of 3.6 Å was in good agreement with the literature value of the interlayer spacing in the stacked sheets model of the melanin (30), which indicated melanin from *C. molossus* L. was composed of oligomers condensed into nanoaggregates instead of the highly cross-linked heteropolymer and there were not other molecules embedding between layers.

An estimate of the average melanin grain size could be obtained from the Debye–Scherrer relationship (31):

$$D = 0.9\lambda/\text{FWHM}.\cos\theta \quad (2)$$

where FWHM is the full width at half maximum of the diffraction peak. The obtained value was 18.1 Å, which supported the nano-aggregate model of melanin. In fact, they might correspond to the lateral or height extension of the melanin stacked sheets protomolecules. In particular, the value $D = 18.1$ Å obtained for melanin from *C. molossus* L. corresponded to about five stacked sheets of planar structures, which was inconsistent with the conclusion reported in the literature that the average dimension of the natural melanin protomolecules was lower than synthetic melanin (4 sheets) (29). This might be because the non-covalent bonds between the layers in the structural units of melanin from *C. molossus* L. were greater, leading to the greater layer bulk density.

XRF analysis The XRF qualitative test result of melanin from *C. molossus* L. is shown in Fig. 8. In addition to the element of S, some metallic elements, especially, more Fe element also existed in the *C. molossus* L. sample, showing its good adsorption

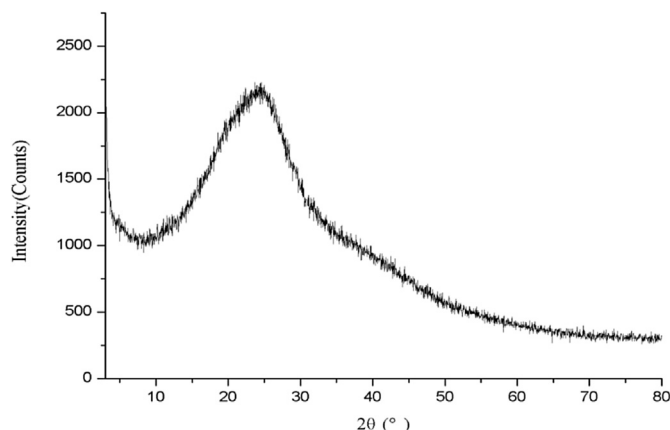


FIG. 7. The XRD patterns of melanin from *Catharsius molossus* L.

properties of metallic elements (32) and the structural units with five stacked sheets were interconnected with each other by the ferric ions to form the sub-structures with the diameter of 10–20 nm in the melanin from *C. molossus* L. (33).

FSEM scanning The results of FSEM (Fig. 9) showed the melanin from *C. molossus* L. consisted of irregularly instead of spherically shaped particles, which was inconsistent with the conclusion drawn by the literature (34) that natural melanin was in spherical shape. In addition, measured by the software, the average particle size of the melanin from *C. molossus* L. was about 1 μm , greater than that of *Sepia* melanin (about 150 nm) (33). Based on the previous conclusion that the advanced structure of melanin was maintained by polypeptides (35), we could infer the difference in the particle size of heterologous melanin was caused by different polypeptides combined with melanin. In particular, when the magnification was 40.00 KX, the particles from *C. molossus* L. sample consisting of tiny layered structures, without non-smooth surface, were clearly observed, which highlighted its complex three-dimensional structure.

MALDI-TOF/TOF-MS analysis MALDI-TOF/TOF-MS spectra of melanin from *C. molossus* L. (Fig. 10) showed the mass-to-charge

ratios (m/z) of fragments varied from 100 to 600, indicating the shape of the advanced structure and sub-structure of melanin were maintained by the non-covalent bonds. The m/z value of the pseudo molecular ion peak was 549, indicating the molecular weight of each layer in the stacked sheets model of the melanin was 548 Da. Hence, the molecular weight of each structural unit (5 sheets) in the *C. molossus* L. sample was 2740 Da. In addition, the m/z ratios of the related fragments were 518, 400, 307, 255, 228, and 212. Combined with results of Py-GC/MS, IR, NMR, the possible chemical structures of melanin from *C. molossus* L. corresponding to the main peaks could be inferred as shown in Fig. 11, which also met the fragmentation regularity of the indole and pyrrole ring by the mass spectrometry (36–39). In particular, chemical groups might be connected to each other through various chemical bonds. The measured ratios of C/H and C/N (mol/mol) for the structure shown in Fig. 11 are 1.28 and 7.75, respectively, close to the theoretical ratios (1.33, 7.62), showing this structure might account for the large proportion in the melanin from *C. molossus* L. There were some unknown ion peaks in the MALDI-TOF/TOF-MS spectra, possibly due to the presence of a small amount of protein and phaeomelanin in the prepared melanin.

Thermal analysis It was interesting to find melanin from *C. molossus* L. was its high thermal stability compared to other natural polymers, as shown in Fig. 12. The TGA and DTG curves showed the weight loss process could be mainly divided into three stages (21.6°C to 132.1°C, 132.1°C to 256.0°C, 256.0°C to 594.0°C) and the weight loss rates were larger at the temperatures of 50.7°C, 226.1°C, 335.1°C. Combined with three less obvious endothermic peaks in the DSC curve, the inference could be made; In the first stage, the loss of free water and bound water in melanin mainly occurred; In the second stage, the advanced structure and sub-structure of melanin and part of the non-covalent bonds between layers in the structural units were destroyed; In the last stage, most non-covalent bonds between layers in the structural units, covalent bonds among the monomers such as indole, pyrrole and their derivatives and part of indole and pyrrole rings were destroyed. So, high temperature might be a good way to purify melanin, which could provide the most favorable help for the exploration of melanin structure. In particular, the weight loss

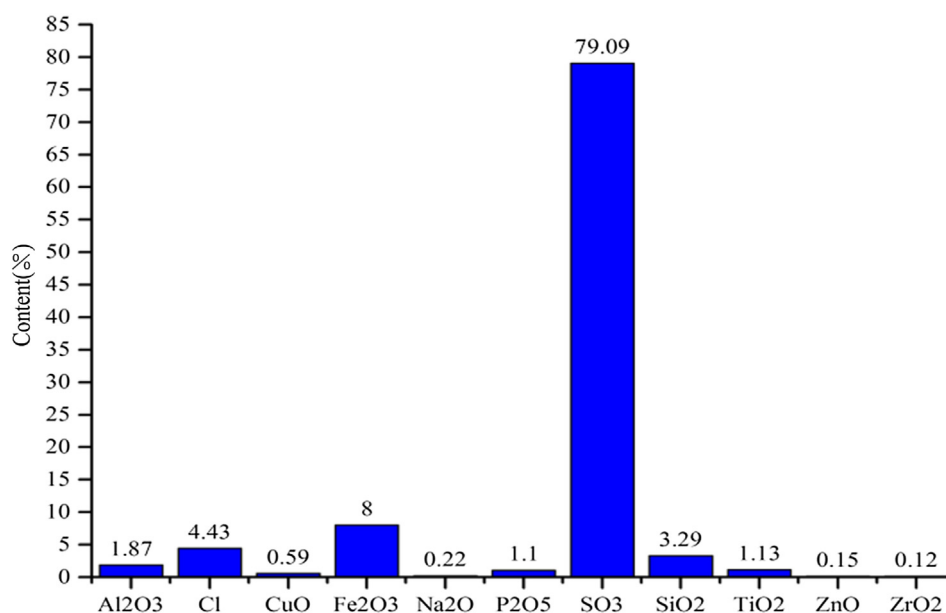
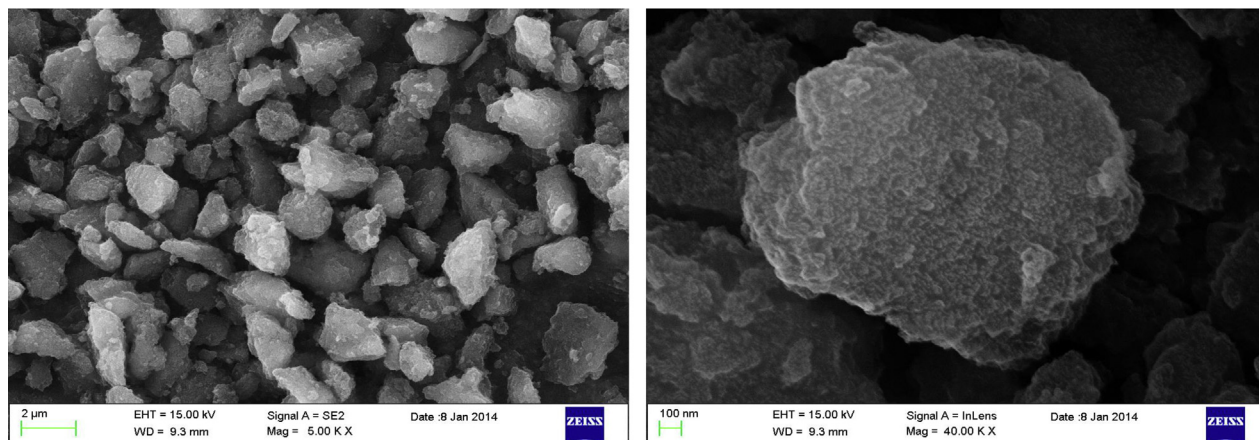
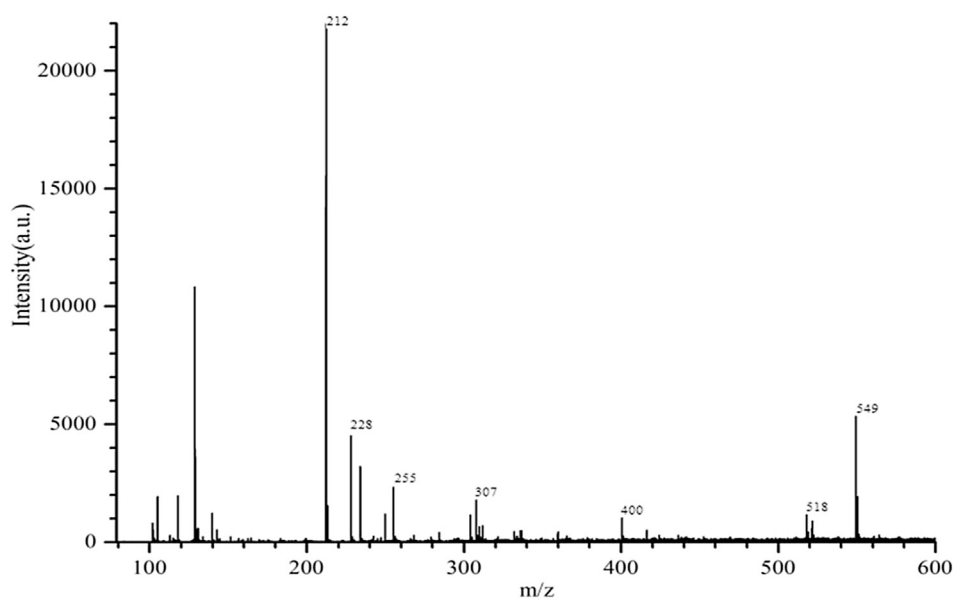
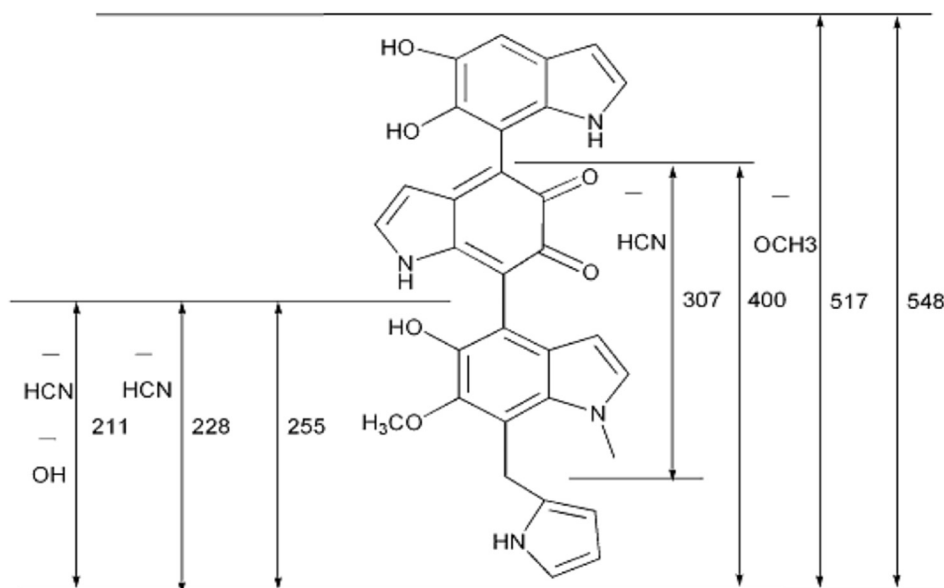
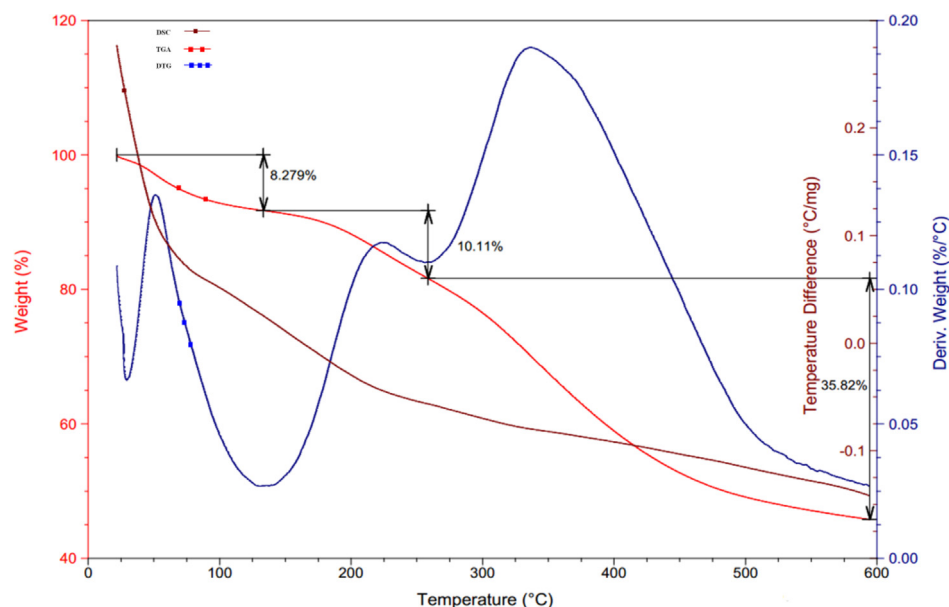


FIG. 8. XRF qualitative test result of melanin from *Catharsius molossus* L.

FIG. 9. FSEM morphologies of melanin from *Catharsius molossus* L.FIG. 10. MALDI-TOF/TOF-MS spectra of melanin from *Catharsius molossus* L.FIG. 11. The possible chemical structures corresponding to the main peaks in the MALDI-TOF/TOF-MS spectra of melanin from *Catharsius molossus* L.

FIG. 12. TGA-DSC-DTG curves of melanin from *Catharsius molossus* L.

was only about 54% of the initial mass of the melanin from *C. molossus* L. until 600°C and this result was not surprising considering this melanin had well-developed graphitic-like structures, capable of supporting such high temperature (40).

Natural melanin was a special class of bioactive substance and it had, in fact, many biological functions such as protection against the degradation of proteins, photoprotection of human cells preventing DNA damage, antibacterial and antiviral (41–43). Especially, specific molecular structure might well explain its biological functions. Unfortunately, the molecular structure of natural melanin was unclear. In this paper, *C. molossus* L. melanin in high purity was prepared using the waste alkali liquor produced by extraction of chitin. Further, its chemical composition and structure was explored by various techniques, finding the high-thermal-stability melanin from *C. molossus* L. was irregular in shape and its structure could be divided into three levels: advanced structure maintained by polypeptides, substructure maintained by the ferric ion and microstructure. Most notably, its microstructure showed the graphite-like layered structure containing five layers linked by non-covalent bonds and each layer mainly consisted of DHI and its derivatives. Thus, various biological functions of natural melanin might be closely linked to its hierarchical structure, especially, advanced structure and substructure, which was similar to the important biomolecule—protein. Future studies were essential to understand the advanced structure and substructure of natural melanin and the structure-function relationship.

ACKNOWLEDGMENTS

This work was financially supported by the Natural Science Foundation of China (no. 30902005), Scientific Research Fund from Education Department of Sichuan Province (no. 13ZB0274), Post-graduate Innovation Fund Project by Southwest University of Science and Technology (nos. 13ycjj47 and 14ycy007).

References

- Wakamatsu, K., Murase, T., Zucca, F. A., Zecca, L., and Ito, S.: Biosynthetic pathway to neuromelanin and its aging process, *Pigment Cell Melanoma Res.*, **25**, 792–803 (2012).
- Vas, G., Vekey, K., Czira, G., Tamas, J., Favretto, D., Traldi, P., Bertazzo, A., Costa, C., and Allegri, G.: Characterization of melanins by pyrolysis/gas chromatography/mass spectrometry, *Rapid Commun. Mass Spectrom.*, **7**, 870–873 (1993).
- Hung, Y. C., Sava, V. M., Makan, S. Y., Chen, T. H. J., Hong, M. Y., and Huang, G. S.: Antioxidant activity of melanins derived from tea: comparison between different oxidative states, *Food Chem.*, **78**, 233–240 (2002).
- El-Obeid, A., Al-Harbi, S., Al-Jomah, N., and Hassib, A.: Herbal melanin modulates tumor necrosis factor alpha (TNF- α), interleukin 6 (IL-6) and vascular endothelial growth factor (VEGF) production, *Phytomedicine*, **13**, 324–333 (2006).
- Hung, Y. C., Sava, V. M., Hong, M. Y., and Huang, G. S.: Inhibitory effects on phospholipase A2 and antivenin activity of melanin extracted from *Thea sinensis* Linn, *Life Sci.*, **74**, 2037–2047 (2004).
- Montefiori, D. C. and Zhou, J.: Selective antiviral activity of synthetic soluble L-tyrosine and L-DOPA melanins against human immunodeficiency virus in vitro, *Antiviral. Res.*, **15**, 11–25 (1991).
- Hung, Y. C., Sava, V. M., Blagodarsky, V. A., Hong, M. Y., and Huang, G. S.: Protection of tea melanin on hydrazine-induced liver injury, *Life Sci.*, **72**, 1061–1071 (2003).
- Dadachova, E., Bryan, R. A., Huang, X., Moadel, T., Schweitzer, A. D., Aisen, P., Nosanchuk, J. D., and Casadevall, A.: Ionizing radiation changes the electronic properties of melanin and enhances the growth of melanized fungi, *PLoS One*, **2**, e457 (2007).
- Ma, J. H., Tan, C. J., Zhao, Y. S., He, F. Y., and Yang, M.: Establishment of fingerprint of active fraction from dried body of *Catharsius molossus* by capillary electrophoresis and analysis by its total quantum statistical moment, *Chin. Herb. Med.*, **44**, 1263–1266 (2013).
- Ma, J. H., Tan, C. J., Deng, X., and Xin, C.: Preparation and preliminary characterization of chitosan from *Catharsius molossus* discards, *J. Chin. Med. Mater.*, **35**, 1029–1032 (2012).
- Ozeki, H., Ito, S., Wakamatsu, K., and Thody, A. J.: Spectrophotometric characterization of eumelanin and pheomelanin in hair, *Pigment Cell Res.*, **9**, 265–270 (1996).
- Pezzella, A., D'Ischia, M., Napollitano, A., Palumbo, A., and Protta, G.: An integrated approach to the structure of *Sepia* melanin. Evidence for a high proportion of degraded 5,6-dihydroxyindole-2-carboxylic acid units in the pigment backbone, *Tetrahedron*, **53**, 8281–8286 (1997).
- Sugumaran, M., Duggaraju, R., Generozova, F., and Ito, S.: Insect melanogenesis. II. Inability of manduca phenoloxidase to act on 5,6-dihydroxyindole-2-carboxylic acid1, *Pigment Cell Res.*, **12**, 118–125 (1999).
- Dworzanski, J. P. and Meuzelaar, H. L. C.: Pyrolysis mass spectrometry methods, p. 1906, in: Lindon, J. C., Tranter, G. E., and Holmes, J. L. (Eds.), *Encyclopedia of spectroscopy and spectrometry*. Elsevier Science, San Diego (2000).
- Latocha, M., Chodurek, E., Kurkiewicz, S., Świątkowska, L., and Wilczok, T.: Pyrolytic GC-MS analysis of melanin from black, gray and yellow strains of *Drosophila melanogaster*, *J. Anal. Appl. Pyrolysis*, **56**, 89–98 (2000).
- Glass, K., Ito, S., Wilby, P. R., Sota, T., Nakamura, A., Bowers, C. R., Vinther, J., Dutta, S., Summons, R., Briggs, D. E. G., Wakamatsu, K., and Simon, J. D.: Direct chemical evidence for eumelanin pigment from the jurassic period, *Proc. Natl. Acad. Sci. USA*, **109**, 10218–10223 (2012).

17. **Stepień, K., Dzierżega-Leczna, A., Kurkiewicz, S., and Tam, I.:** Melanin from epidermal human melanocytes: study by pyrolytic GC/MS, *J. Am. Soc. Mass Spectrom.*, **20**, 464–468 (2009).
18. **Bleasel, M. D., Aldous, S., and Davies, N. W.:** Distinction between melanins derived from different precursors using pyrolysis/gas chromatography/mass spectrometry and the NIST mass spectral search algorithm, *J. Anal. Appl. Pyrolysis*, **70**, 649–663 (2003).
19. **Dzierżega-Leczna, A., Kurkiewicz, S., Stepień, K., Chodurek, E., Riederer, P., and Gerlach, M.:** Structural investigations of neuromelanin by pyrolysis-gas chromatography/mass spectrometry, *J. Neural Transm.*, **113**, 729–734 (2006).
20. **Corradoini, M. G., Napolitano, A., and Protà, G.:** A biosynthetic approach to the structure of eumelanins. The isolation of oligomers from 5,6-dihydroxy-1-methylindole, *Tetrahedron*, **42**, 2083–2088 (1986).
21. **Takaya, Y., Uchisawa, H., Narumi, F., and Matsue, H.:** Illexins A, B, and C from squid ink should have a branched structure, *Biochem. Biophys. Res. Commun.*, **226**, 335–338 (1996).
22. **Ito, S. and Fujita, K.:** Microanalysis of eumelanin and pheomelanin in hair and melanomas by chemical degradation and liquid chromatography, *Anal. Biochem.*, **144**, 527–536 (1985).
23. **Pierce, J. A. and Rast, D. M.:** A comparison of native and synthetic mushroom melanins by Fourier-transform infrared spectroscopy, *Phytochemistry*, **39**, 49–55 (1995).
24. **Katritzky, A. R., Akhmedov, N. G., Denisenko, S. N., and Denisko, O. V.:** ¹H NMR spectroscopic characterization of solutions of *Sepia* melanin, *Sepia* melanin free acid and human hair melanin, *Pigment Cell Res.*, **5**, 93–97 (2002).
25. **Bronze-Uhle, E. S., Batagin-Neto, A., Xavier, P. H. P., Fernandes, N. I., de Azevedo, E. R., and Graeff, C. F. O.:** Synthesis and characterization of melanin in DMSO, *J. Mol. Struct.*, **1047**, 102–108 (2013).
26. **Adhyaru, B. B., Akhmedov, N. G., Katritzky, A. R., and Bowers, C. R.:** Solid-state cross-polarization magic angle spinning ¹³C and ¹⁵N NMR characterization of *Sepia* melanin, *Sepia* melanin free acid and human hair melanin in comparison with several model compounds, *Magn. Reson. Chem.*, **41**, 466–474 (2003).
27. **Duff, G. A., Roberts, J. E., and Foster, N.:** Analysis of the structure of synthetic and natural melanins by solid-phase NMR, *Biochemistry*, **27**, 7112–7116 (1988).
28. **Moses, D. N., Harreld, J. H., Stucky, G. D., and Waite, J. H.:** Melanin and *Glycera* jaws emerging dark side of a robust biocomposite structure, *J. Biol. Chem.*, **281**, 34826–34832 (2006).
29. **Capozzi, V., Perna, G., Carmone, P., Gallone, A., Lastella, M., Mezzenga, E., Quartucci, G., Ambrico, M., Agugli, V., Biagi, P. F., and other 5 authors:** Optical and photoelectronic properties of melanin, *Thin Solid Films*, **511**, 362–366 (2006).
30. **Clancy, C. M. and Simon, J. D.:** Ultrastructural organization of eumelanin from *Sepia officinalis* measured by atomic force microscopy, *Biochemistry*, **40**, 13353–13360 (2001).
31. **Klug, H. P. and Alexander, L. E.:** X-ray diffraction procedures. Wiley, New York (1974).
32. **Potts, A. M. and Au, P. C.:** The affinity of melanin for inorganic ions, *Exp. Eye Res.*, **22**, 487–491 (1976).
33. **Liu, Y. and Simon, J. D.:** Isolation and biophysical studies of natural eumelanins: applications of imaging technologies and ultrafast spectroscopy, *Pigment Cell Res.*, **18**, 42–48 (2005).
34. **Nofsinger, J. B., Forest, S. E., Eibest, L. M., Gold, K. A., and Simon, J. D.:** Probing the building blocks of eumelanins using scanning electron microscopy, *Pigment Cell Res.*, **13**, 179–184 (2000).
35. **Sharma, S., Wagh, S., and Govindarajan, R.:** Melanosomal proteins—role in melanin polymerization, *Pigment Cell Res.*, **15**, 127–133 (2002).
36. **Ernö, P., Philippe, B., and Martin, B.:** Structure determination of organic compounds, 4th ed. Springer, New York (2009).
37. **Seraglia, R., Trald, P., Elli, G., Bertazzo, A., Costa, C., and Allegri, G.:** Laser desorption/ionization mass spectrometry in the study of natural and synthetic melanins. I—Tyrosine melanins, *Biol. Mass Spectrom.*, **22**, 687–697 (1993).
38. **Napolitano, A., Pezzella, A., Protà, G., Seraglia, R., and Traldi, P.:** Structural analysis of synthetic melanins from 5,6-dihydroxyindole by matrix-assisted laser desorption/ionization mass spectrometry, *Rapid Commun. Mass Spectrom.*, **10**, 468–472 (1996).
39. **Pezzella, A., Napolitano, A., D'Ischia, M., Protà, G., Seraglia, R., and Traldi, P.:** Identification of partially degraded oligomers of 5,6-dihydroxyindole-2-carboxylic acid in *Sepia* melanin by matrix-assisted laser desorption/ionization mass spectrometry, *Rapid Commun. Mass Spectrom.*, **11**, 368–372 (1997).
40. **Deziderio, S. N., Brunello, C. A., da Silva, M. I. N., Cotta, M. A., and Graeff, C. F. O.:** Thin films of synthetic melanin, *J. Non-Cryst. Solids*, **338**, 634–638 (2004).
41. **Riley, P. A.:** *Materia melanica: further dark thoughts*, *Pigment Cell Res.*, **5**, 101–106 (1992).
42. **Cesarini, J.:** Photo-induced events in the human melanocytic system: photo-aggression and photoprotection, *Pigment Cell Res.*, **1**, 223–233 (1988).
43. **Dong, C. H. and Yao, Y. J.:** Isolation, characterization of melanin derived from *Ophiocordyceps sinensis*, an entomogenous fungus endemic to the Tibetan Plateau, *J. Biosci. Bioeng.*, **113**, 474–479 (2012).